# Higher velocity, high-foot implosions on the National Ignition Facility lasera)

D. A. Callahan, O. A. Hurricane, D. E. Hinkel, T. Döppner, T. Ma, H.-S. Park, M. A. Barrios Garcia, L. F. Berzak Hopkins, D. T. Casey, C. J. Cerjan, E. L. Dewald, T. R. Dittrich, M. J. Edwards, S. W. Haan, A. V. Hamza, J. L. Kline, J. P. Knauer, A. L. Kritcher, O. L. Landen, S. LePape, A. G. MacPhee, J. L. Milovich, A. Nikroo, A. E. Pak , P. K. Patel, J. R. Rygg, J. E. Ralph, J. D. Salmonson, B. K. Spears, P. T. Springer, R. Tommasini, L. R. Benedetti, R. M. Bionta, E. J. Bond, D. K. Bradley, J. A. Caggiano, J. E. Field, D. N. Fittinghoff, J. Frenje, M. Gatu Johnson, G. P. Grim, R. Hatarik, F. E. Merrill, S. R. Nagel, N. Izumi, S. F. Khan, R. P. J. Town, D. B. Sayre , P. Volegov, and C. H. Wilde

Citation: Physics of Plasmas (1994-present) **22**, 056314 (2015); doi: 10.1063/1.4921144
View online: http://dx.doi.org/10.1063/1.4921144
View Table of Contents: http://scitation.aip.org/content/aip/journal/pop/22/5?ver=pdfcov
Published by the AIP Publishing



# Higher velocity, high-foot implosions on the National Ignition Facility laser[a)]

D. A. Callahan,[1,b)] O. A. Hurricane,[1] D. E. Hinkel,[1] T. Döppner,[1] T. Ma,[1] H.-S. Park,[1] M. A. Barrios Garcia,[1] L. F. Berzak Hopkins,[1] D. T. Casey,[1] C. J. Cerjan,[1] E. L. Dewald,[1] T. R. Dittrich,[1] M. J. Edwards,[1] S. W. Haan,[1] A. V. Hamza,[1] J. L. Kline,[2] J. P. Knauer,[3] A. L. Kritcher,[1] O. L. Landen,[1] S. LePape,[1] A. G. MacPhee,[1] J. L. Milovich,[1] A. Nikroo,[4] A. E. Pak,[1] P. K. Patel,[1] J. R. Rygg,[1] J. E. Ralph,[1] J. D. Salmonson,[1] B. K. Spears,[1] P. T. Springer,[1] R. Tommasini,[1] L. R. Benedetti,[1] R. M. Bionta,[1] E. J. Bond,[1] D. K. Bradley,[1] J. A. Caggiano,[1] J. E. Field,[1] D. N. Fittinghoff,[1] J. Frenje,[5] M. Gatu Johnson,[5] G. P. Grim,[2] R. Hatarik,[1] F. E. Merrill,[2] S. R. Nagel,[1] N. Izumi,[1] S. F. Khan,[1] R. P. J. Town,[1] D. B. Sayre,[1] P. Volegov,[2] and C. H. Wilde[2]

[1]*Lawrence Livermore National Laboratory, Livermore, CA 94551, USA*
[2]*Los Alamos National Laboratory, Los Alamos, NM 87545, USA*
[3]*Laboratory for Laser Energetics, University of Rochester, Rochester, NY 14623, USA*
[4]*General Atomics, San Diego, CA 92121, USA*
[5]*Massachusetts Institute of Technology, Cambridge, MA 02139, USA*

(Received 31 December 2014; accepted 24 February 2015; published online 15 May 2015)

By increasing the velocity in "high foot" implosions [Dittrich *et al.*, Phys. Rev. Lett. **112**, 055002 (2014); Park *et al.*, Phys. Rev. Lett. **112**, 055001 (2014); Hurricane *et al.*, Nature **506**, 343 (2014); Hurricane *et al.*, Phys. Plasmas **21**, 056314 (2014)] on the National Ignition Facility laser, we have nearly doubled the neutron yield and the hotspot pressure as compared to the implosions reported upon last year. The implosion velocity has been increased using a combination of the laser (higher power and energy), the hohlraum (depleted uranium wall material with higher opacity and lower specific heat than gold hohlraums), and the capsule (thinner capsules with less mass). We find that the neutron yield from these experiments scales systematically with a velocity-like parameter of the square root of the laser energy divided by the ablator mass. By connecting this parameter with the inferred implosion velocity ($v$), we find that for shots with primary yield $>1 \times 10^{15}$ neutrons, the total yield $\sim v^{9.4}$. This increase is considerably faster than the expected dependence for implosions without alpha heating ($\sim v^{5.9}$) and is additional evidence that these experiments have significant alpha heating. © *2015 AIP Publishing LLC*. [http://dx.doi.org/10.1063/1.4921144]

## I. INTRODUCTION

In indirect drive inertial confinement fusion (ICF), a layer of deuterium-tritium (DT) fuel is surrounded by a thin ($\sim$165–195 $\mu$m thick) CH shell with outer radius $\sim$1.1 mm or other ablator material such with similar areal density. The capsule is placed inside a cylindrical hohlraum. Laser beams enter the hohlraum through holes in the ends of the cylinder and strike the high Z (gold or depleted uranium (DU)) walls of the hohlraum and are converted to x-rays. The x-rays ablate the surface of the capsule and implode the capsule to reach the necessary temperature and density conditions needed to produce fusion.

In the "high foot" campaign,[1–4] the laser pulse shape is chosen to deliberately put the capsule on a higher adiabat by launching a stronger first shock. In both calculations[1,4,5] and experiments,[6,7] this choice of high foot reduces the amount of ablation front instability growth. In turn, this reduces the potential for instabilities that bring higher Z ablator (CH plastic) into the hotspot, which cools the hotspot and reduces neutron yield. The higher adiabat does come at a price, since it reduces the ultimate amount of compression that can be achieved. This trade off between 1-D performance (compression) and 2-D stability results in a less optimal 1-D design but one that is less stressing and easier to calculate and thus easier to achieve in reality. Our goal in this campaign was to find a design that performed similar to simulations and then push that design until we found a cliff in performance to study failure modes.

In ICF implosions, performance is a strong function of the fuel velocity, since fuel velocity provides the energy for PdV work on the hotspot. The ignition threshold factor (ITF), which is a measure of how close we are to ignition, scales as the fuel velocity to the 8th power[8,9]

$$ITF \sim v^8 \alpha^{-4} S \left(\frac{\Delta R}{R}\right) \left(\frac{M_{clean}}{M_{DT}}\right)^{0.5},$$

where $v$ is the implosion velocity, $\alpha$ is the fuel adiabat, $S$ is a hotspot shape term that depends on the deviation from round ($\Delta R/R$—where R is the hotspot radius), and ($M_{clean}/M_{DT}$) is the fraction of the fuel mass that is "clean" (not mixed with ablator material). This strong dependence on fuel velocity motivates us to work on increasing the fuel velocity of the implosions—however, this must be done keeping both hotspot shape and mix under control.

In this paper, we will discuss our efforts to increase the implosion velocity. In Sec. II, we will discuss the methods for increasing velocity and increase in performance with

[a)]Paper PI1 1, Bull. Am. Phys. Soc. **59**, 235 (2014).
[b)]Invited speaker.

 

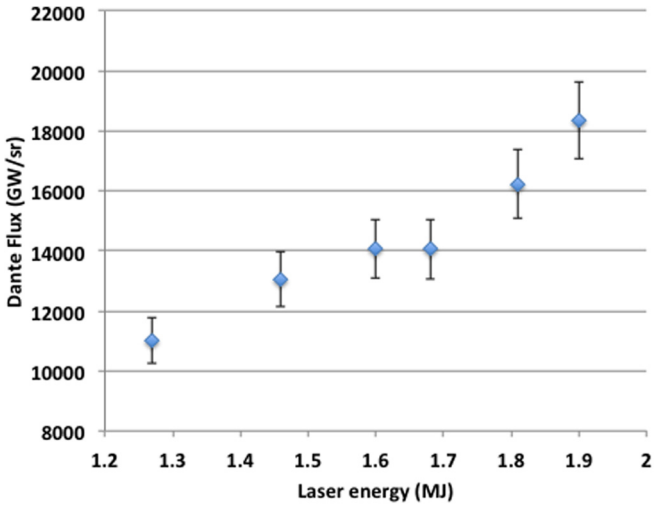


FIG. 1. Peak drive, as measured by the Dante diagnostic, increases linearly with input laser energy.

increasing velocity. In Sec. III, we will show that the implosion hotspot changes in a systematic way as we change the laser, hohlraum, and capsule. In Sec. IV, we will connect performance to an estimate of the implosion velocity.

## II. METHODS FOR INCREASING IMPLOSION VELOCITY

We have explored three methods for increasing the implosion velocity—increasing the laser energy and power, using depleted uranium hohlraums, and reducing the thickness of the ablator.

Increasing the laser energy and power increases the radiation drive inside the hohlraum and results in a higher flux on the capsule. Our experiments have ranged in energy from 1.3 MJ up to 1.9 MJ and laser powers ranging from 350 TW to 440 TW. For these experiments, we measure the x-ray drive using the Dante diagnostic[10] and find approximately a linear relationship between the measured peak flux and the input laser energy as is shown in Figure 1. Although the absorbed laser energy—input minus the backscatter—would be a better metric, we report the input laser energy because some of the backscatter diagnostics are to be turned off during high yield shots to prevent damage to the diagnostic. Given that the fraction of energy backscattered across shots tends to be very similar, this is a reasonable approximation to make.

We should note that while we have gone up to 1.9 MJ of laser energy, we have not pushed to NIF's limits on laser power (>500 TW has been demonstrated).[11] This is because we find that the hotspot shape becomes more oblate "pancaked" (which reduces the efficiency of converting PdV work into internal energy of the hotspot[12]) as the laser power is increased as is shown in Figure 2.

The second method of increasing the fuel velocity is by using depleted uranium hohlraums. As was done previously,[13] we use a hohlraum that is a sandwich of gold and uranium. The hohlraum is made from about 7 $\mu$m of DU with an inner layer of 0.7 $\mu$m thick gold. The gold layer serves three purposes: (1) it provides a barrier to prevent oxidation of the DU, (2) it keeps the drive in the foot the same for gold and uranium hohlraums so that the shock timing stays the same between the two hohlraum materials (in fact, the opacity of gold is higher than uranium at foot temperatures, but does not significantly impact the hohlraum energetics because the amount of energy in the foot is relatively small), and (3) the laser energy is deposited in this gold layer so that the laser produced portion of the drive spectrum stays the same for gold and uranium hohlraums. This allows us to switch from gold hohlraums to uranium hohlraums with the same shock timing and spectrum but with higher drive. The outside of the hohlraum wall is composed of another ~25 $\mu$m of gold for structural support.

Depleted uranium has higher opacity and lower specific heat than gold hohlraums at peak drive temperatures (~300 eV).[14] This results in less energy going into the hohlraum wall. Since approximately 50% of the energy in a hohlraum ends up in the wall, changes in wall materials can significantly impact the drive on the capsule. We have found in previous experiments,[13,15] that depleted uranium hohlraums give ~6.5% more drive on the capsule than an equivalent gold hohlraum, when driven with the same laser power profile.

In previous experiments (using a low foot drive) comparing gold and uranium hohlraums,[13] both implosions were

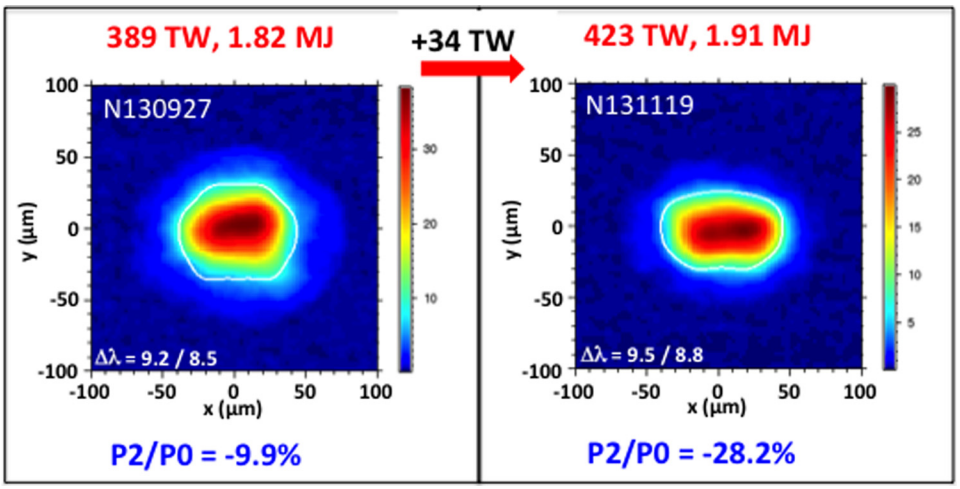


FIG. 2. Implosion hotspot shape, as measured by hotspot x-ray emission, becomes more oblate ("pancaked") as the laser power is increased. This effect limited the peak power used in these experiments to ~425 TW.

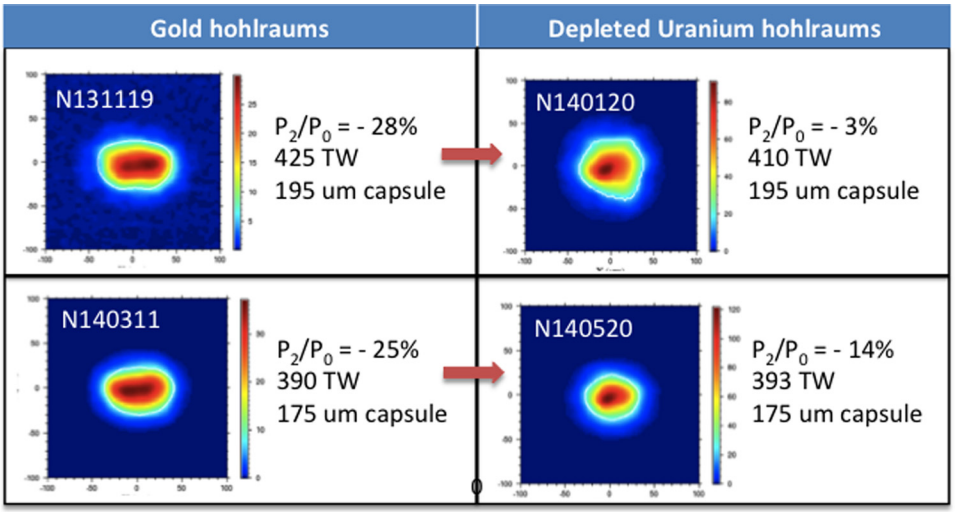


FIG. 3. Implosion shape becomes less oblate ("pancaked") using a depleted uranium hohlraum rather than a gold hohlraum. This is likely due to the higher opacity of uranium than gold. However, both implosions have large amounts of crossbeam energy transfer so a change in crossbeam transfer could contribute.

prolate ("sausaged") in hotspot shape making it difficult to assess the impact of DU hohlraums on shape. In this series of experiments, we find that DU hohlraums show an improvement in hotspot Legendre mode $P_2$ shape with uranium giving an additional 6.5–8 $\mu$m of $P_2$ when compared to gold hohlraums.[15] Figure 3 shows two pairs of DT experiments showing the hotspot shape improvement when using a DU hohlraum. The higher hohlraum wall opacity is likely to be the cause of this improvement in $P_2$; however, since there is significant crossbeam energy transfer,[16] it is also possible that the improvement is due to changes in plasma conditions leading to a change in crossbeam energy transfer.

The third method for increasing the implosion velocity was using a thinner capsule. For the same drive, a thinner capsule has less payload (mass), which results in a faster implosion, but has higher in-flight aspect ratio that potentially makes it more susceptible to hydrodynamic instabilities. The optimum capsule thickness requires a balance between velocity and the amount of mass remaining. A capsule that is too thick will be slow for a given laser energy. A capsule that is too thin can suffer two problems: (1) the remaining ablator no longer provides a standoff to prevent for hydrodynamics instabilities at the ablation front from injecting ablator material into the fuel and hotspot, (2) the drive can burn through the ablator and cause a drop in performance[17] due to reduced inertial confinement.

The majority of the high foot experiments have been done with a 195 $\mu$m thick plastic (CH) ablator. This is the same capsule that has been used in many of the "low foot" experiments on the NIF laser. To increase the implosion velocity, we have also conducted experiments with 175 $\mu$m and 165 $\mu$m thick ablators.[18] Since implosion velocity scales like $\sqrt{1/m}$, where $m$ is the capsule mass, we expect that a 10% thinner capsule will give about 5.4% faster implosion velocity for the same drive.

In layered DT implosions, we find that increasing the implosion velocity by each of these three methods improves neutron yield, as is shown in Figure 4. This plot shows all high foot DT implosions with the same hohlraum, fielding conditions, and drive in the foot of the pulse. Excluded from the data set are N130530 (very large, low mode asymmetry in the fuel layer), N130802 (different hohlraum length), N140511 (different fielding conditions), and N141008 (different drive in the foot). (NIF shots are identified by date using a format of NYYMMDD) For these shots, we plot the primary neutron yield (number of neutrons between 13 and 15 MeV) as a function of gold-equivalent laser energy. For experiments using uranium hohlraums, the laser energy has been increased by a factor of 1.065—corresponding to the increase in drive for the uranium hohlraum.[11] The highest performing shots are all in DU hohlraums. The data fall into three curves corresponding to the three capsule thicknesses tested. This shows that as the capsule mass decreases, we improve performance for a given laser energy.

The one outlier in the data set is an experiment conducted on 8/19/14 (N140819) which used the thinnest capsule (165 $\mu$m thick ablator), in a DU hohlraum, driven with 1.77 MJ of laser energy at 390 TW peak power (1.88 MJ Au-equivalent laser energy). Although the yield did

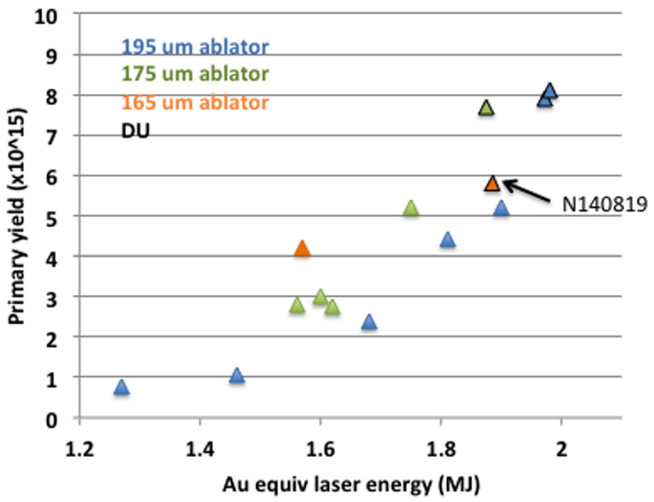


FIG. 4. Neutron yield increases with increased x-ray drive on the capsule [via increasing laser energy and depleted uranium hohlraums (points outlined in black)] and as we make the capsule ablator thinner. The outlier point is the shot N140819, which was the thinnest ablator driven at 1.77 MJ in a depleted uranium hohlraum, but also included a significant defect in the capsule.

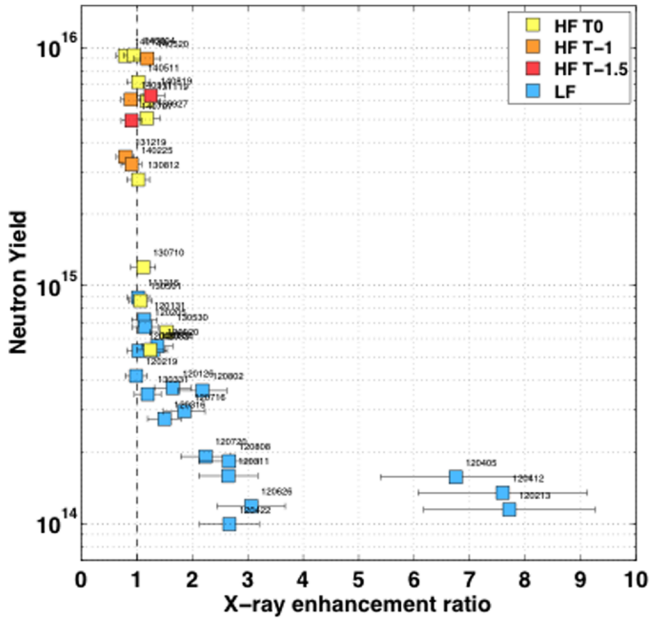


FIG. 5. In spite of high drive and thinner ablators (T0 = 195 $\mu$m, T-1 = 175 $\mu$m, and T-1.5 = 165 $\mu$m thick ablators), there is no evidence of mix of the CH ablator into the hotspot for any of the high foot (HF) shots as measured by x-ray enhancement ratio (high x-ray enhancement means more mix). This includes shot N140819, which used the thinnest capsule (165 $\mu$m), was driven with 1.77 MJ of laser energy in a depleted uranium hohlraum and showed reduced performance.

increase from the previous 165 $\mu$m thick capsule, it falls below the yield for the thicker 175 $\mu$m capsule and below the trend from the other data points.

As mentioned in the Introduction, one of our goals was to push a high foot implosion until we found a cliff in performance and we succeeded in doing so with this shot. The next question is which cliff did we find?

The first place to look is for evidence of ablator mix into the hotspot. A method that has been developed to measure mix into the hotspot is to compare the x-ray yield of the capsule to the x-ray yield that would be expected given the neutron yield and hotspot temperature. Because the CH ablator has higher Z than DT, we would expect hot CH to radiate more energy via bremsstrahlung than hydrogen (DT) and result in a higher x-ray yield than expected.[19] Figure 5 shows the neutron yield as a function of the x-ray ratio for this set of shots—an x-ray ratio of one means no signature of mix into the hotspot. Within the error bars of this measurement technique, all of the high foot shots are "clean" with little to no evidence of hotspot mix.

Another possibility is that we burned through the ablator with the thin capsule and high drive. We have a measure of the total areal density $\rho$r of the CH ablator using the Gamma Reaction History (GRH) diagnostic by measuring the $\gamma$-ray signal from inelastic neutron scattering of $^{12}$C in the ablator material.[20] The N140819 shot showed the lowest carbon $\rho$r of any high foot shot. In addition, the capsule x-ray spectrum measured by the Ross pair filters[21,22] can be fit to infer an optical depth ($\kappa\rho$r). Again, we infer the lowest optical depth for any high foot shot for N140819. Although the calculations suggest that we have 4%–5% of the ablator mass remaining at peak velocity, the experimental evidence suggests that the ablator burned through on this shot.

One way to reconcile the ablator mass remaining with the experimental observation would be if there were significant $\rho$r variations in the shell so that the ablator could burn through on the "thin spots." Two sources for additional $\rho$r variations on this shot are the capsule support tent (45 nm plastic sheets that hold the capsule in the center of the hohlraum), and distortions in the initial shell (described below).

With the thinner capsule, we would expect that the tent would become a larger perturbation because there is less ablator material between the instability growth at the ablation front and the fuel/hotspot. In low foot implosions, we did see evidence of perturbations from the tent.[23] The tent causes density perturbations in the capsule in the region where the tent lifts off of the surface; as such, we expect to see density perturbations on the diagonal relative to the hohlraum axis. As is shown in Figure 6, in this implosion hotspot, we see some "pinching" of the hotspot. Detailed simulations show that the tent produces a jet of material into the hotspot and leaves behind a region of low $\rho$r. Thin spots from the tent, coupled with the high drive, could have resulted in ablator burn through in parts of the capsule.

A second potential reason for low ablator $\rho$r is a defect in this particular capsule. While the ablator thickness was uniform when the capsule was chosen, a 3 $\mu$m peak-to-valley perturbation in the shell radius near the fill tube was detected during the formation of the DT layer. (The fill tube is the tube that allows us to fill the capsule with DT fuel. Since this shot, it has been determined that the "wrinkle" in the shell was due to UV light that is used to cure the glue that holds the fill tube in place and a new process is in place to avoid

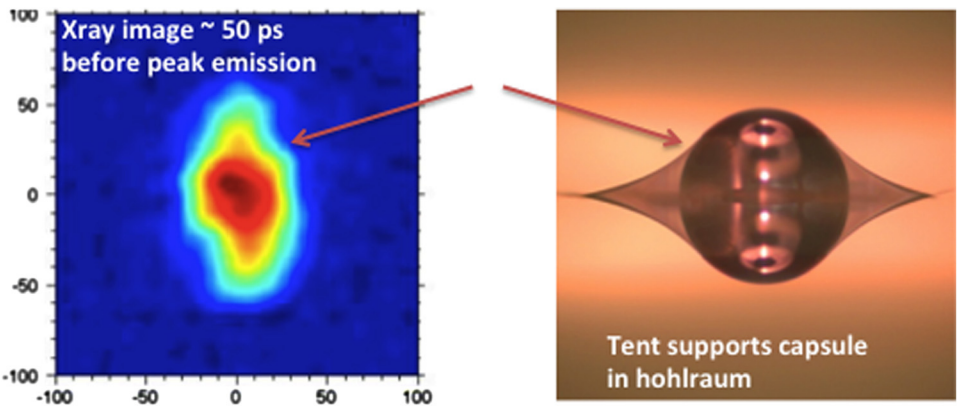


FIG. 6. X-ray hotspot emission for the N140819 shot (165 $\mu$m capsule driven by 1.77 MJ in a depleted uranium hohlraum) shows some signs of "pinching" off near the location of the support tent. As the capsule was thin and the drive was high, the support tent may have produced thin spots in the imploded DT fuel layer.

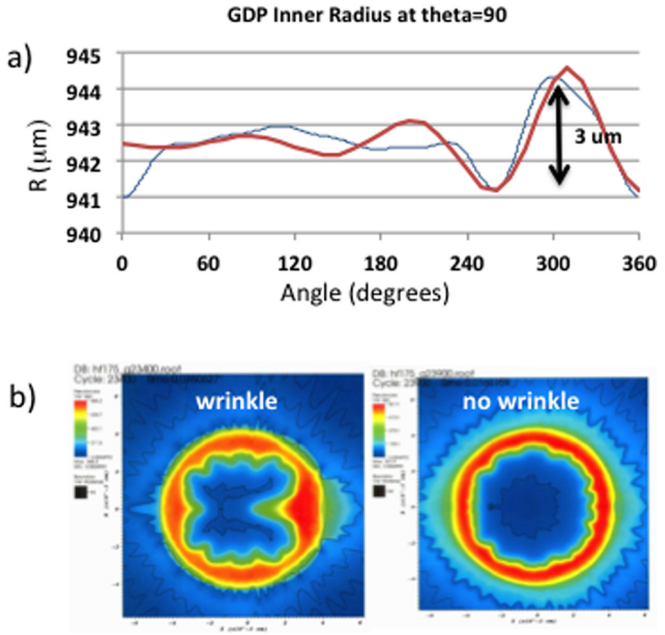


FIG. 7. (a) Capsule for the N140819 shot had a 3 $\mu$m defect in the ablator shell ("wrinkle"). (b) Simulations accounting for the "wrinkle" show thin spots in the shell density but show little impact on neutron yield.

this in future.) Simulations of this perturbation, shown in Figure 7, show that the defect produces thin regions in the imploded core. The simulations show a small reduction in neutron yield (~10%) from this perturbation—however, the thin spot created by this perturbation could also contribute to the ablator burn through.

In future, we plan to repeat this experiment with a better capsule and with slightly reduced drive (less laser energy) to better determine the location of the "cliff" in performance. For the remaining analysis, we will not include the N140819 shot since it clearly does not follow the same scaling as the other shots.

## III. PERFORMANCE SCALING WITH VELOCITY-LIKE PARAMETER

What can we learn from looking at this dataset as a whole? The goal here is to try to understand trends in the data and consistency in the data using experimental measurements as much as possible. One way to collapse the yield data in Figure 8 is to plot them against $\sqrt{E_{Au}A/m}$, where $E_{Au}$ is the gold equivalent laser energy (increase by laser energy by 1.065 for uranium hohlraums, as described above), $A$ is the initial capsule surface area (this is a small correction but used because some of the capsules were smaller based on the capsule fabrication mandrels used), and $m$ is the ablator mass. All three of the parameters are quantities that we directly measure for each shot. $(E_{Au}\ A)$ can be thought of as proportional to a capsule absorbed energy. This means that this quantity, $\sqrt{E_{Au}A/m}$, is a velocity like parameter (square root of energy/mass). Because this is not the true velocity, we will use this parameter but normalize to one of the early DT shots (N130812).

The advantage of using $\sqrt{E_{Au}A/m}$ is that it is a quantity that is based on measurements for each experiment (the only inferred quantity is the factor to compensate for uranium hohlraum, as we discussed earlier). Of course, it would be best if we had a direct measure of the fuel velocity for every experiment, but we do not have such a measurement. In Sec. IV, we will discuss the connection between $\sqrt{E_{Au}A/m}$ with an estimate of the fuel velocity that is derived from a measurement of the center of mass velocity and then coupled with calculations infer a fuel velocity for each DT experiment.

Figure 8 shows the total yield for the high foot dataset plotted against this velocity-like parameter. We see that the data from the different capsule thicknesses collapse onto one curve. Plotting on a log-log scale, we see that with the exception of the lowest point, all fall on a straight line. This indicates a power law form, $Y \sim \tilde{v}^p$, where $\tilde{v} \sim \sqrt{E_{Au}A/m}$. If we fit all the data points, the best fit is a power law with $p = 11$. If we exclude the lowest point (which was a low energy shot that did not show much alpha heating), the best fit is a power law with $p = 12.75$. If we fit only the five highest performing shots, the best fit is a power law with $p = 15.75$. However, the three of the five highest performing shots are in uranium hohlraums and as a result, this fit is sensitive to the 1.065 boost that we have used for uranium hohlraums.

We also see a good correlation between $\tilde{v} \sim \sqrt{E_{Au}A/m}$ and the ion temperatures, as is shown in Figure 9. Here, we plot both the ion temperature from the DT neutron peak as

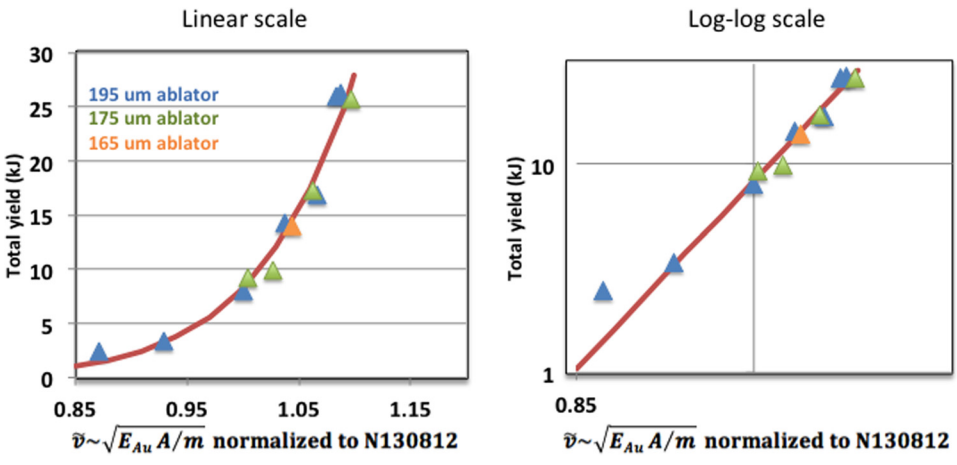


FIG. 8. Yield data collapse on to one curve when plotted against a "velocity-like parameter" $\tilde{v} \sim \sqrt{E_{Au}A/m}$, where $E_{Au}$ is the gold equivalent laser energy (increase in the laser energy by 1.065 for uranium hohlraums), $A$ is the initial capsule surface area, and $m$ is the ablator mass. Curves show, $Y \sim \tilde{v}^{12.75}$, which is the best fit to the data excluding the lowest point.

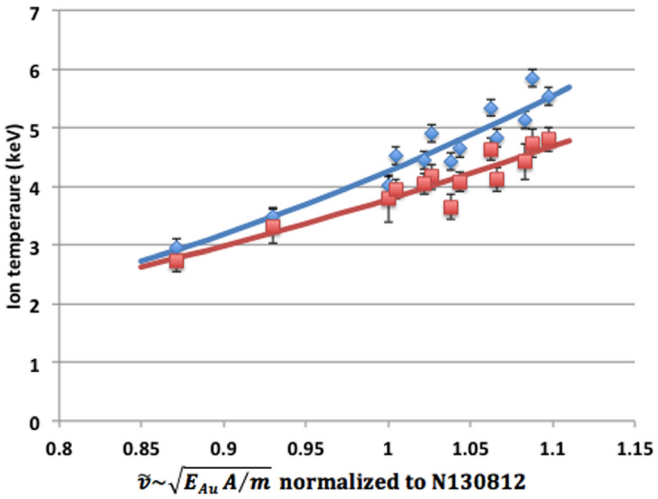


FIG. 9. Ion temperature data plotted against the velocity-like parameter, $\tilde{v} \sim \sqrt{E_{Au}A/m}$. DT ion temperature (blue) scales like $\tilde{v}^{2.8}$, while the DD ion temperature (red) scales like $\tilde{v}^{2.25}$.

well as the ion temperature from the DD neutron peak. We find that the best fit to the data shows that the DT ion temperature scales $\sqrt{E_{Au}A/m}$ to the 2.8 power while the DD ion temperatures scale with the 2.25 power. One of the mysteries of the high foot database is the divergence of the DD and DT ion temperatures, which may be a reflection of non-radial flows in the neutron producing region or other physics.[24,25]

An overall measure of our performance is the hotspot pressure, which is inferred from the experimentally measured yield, hotspot volume, ion temperature, and burn duration.[31] Figure 10 shows a plot of the hotspot pressure as a function of the "coasting" time (i.e., stagnation time ("bangtime") minus the time of end of the laser pulse). Smaller coasting time means that we continue driving the capsule throughout the implosion. The best performing shot

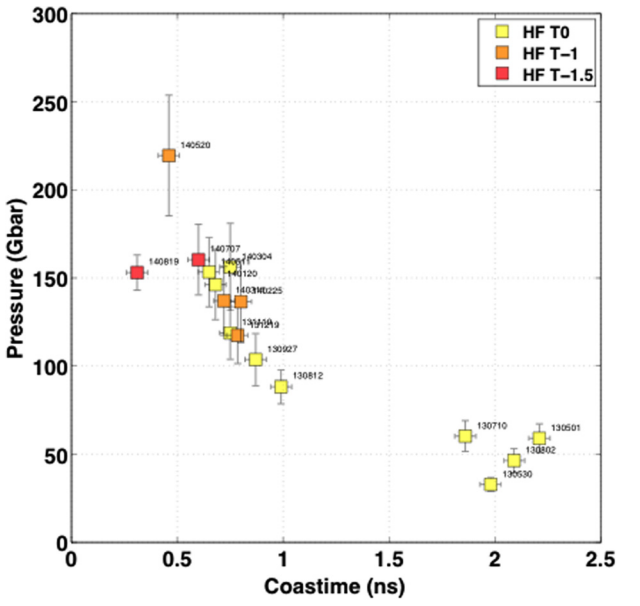


FIG. 10. Hotspot pressure inferred from the data as a function of "coasting" time (bangtime—time of the end of the laser pulse) shows that our highest performing shot (N140520, 175 $\mu$m thick ablator driven with 1.76 MJ in a depleted uranium hohlraum) has a pressure in excess of 200 Gbar.

(N140520—a 175 $\mu$m thick ablator in a DU hohlraum driven with 1.76 MJ at 390 TW) has a pressure in excess of 200 Gbar. It is also evident from this plot that N140819 (thinnest capsule—165 $\mu$m thick—pushed with 1.77 MJ in a uranium hohlraum and discussed in Sec. II) has lower than expected performance. Future experiments will seek to further pinpoint the cliff in performance by pushing our highest performing shot (N140520) with higher power and energy, and reducing the power and energy for the shot (N140819) that went over the cliff.

## IV. CONNECTING TO VELOCITY

As mentioned earlier, plotting quantities against $\tilde{v} \sim \sqrt{E_{Au}A/m}$ is convenient because it is a quantity made up of parameters that are directly measured for each shot. This makes it useful as a metric to compare experiments and plan future experiments. However, for understanding what the data are telling us, we need to connect this parameter to the fuel implosion velocity.

We conducted dedicated experiments using the "convergent ablator" technique to measure the shell center of mass velocity and the amount of ablator remaining.[26] For the high foot, we have done two such experiments. The first, N130409, was a low energy and low power pulse (1.3 MJ, 350 TW). This pulse was a "coasting" pulse where the laser was turned off while the capsule was still at large radius (~600 $\mu$m out of 1100 $\mu$m initial radius). The second was N140601, which was done at high power and energy (1.65 MJ, 380 TW). In this experiment, the laser was kept on until the capsule radius was considerably smaller (~350 $\mu$m—"no coast" pulse). Our experience is keeping the laser on until the capsule is at small radius improves velocity and keeps the shell compressed. Both used the nominal, 195 $\mu$m, capsule ablator thickness. From these experiments, we measure a center of mass velocity and mass remaining in the method described by Hicks.[26] For the thinner ablators (175 $\mu$m and 165 $\mu$m), we have not done convergent ablator experiments, but use data from a two-dimensional inflight measurement, which gives more limited data on velocity and mass remaining but also provides data on inflight implosion shape.[27]

Given the center of mass velocity and mass remaining, we can estimate the fuel velocity using the procedure described by Meezan.[28] This involves several corrections to the data. First, a correction is needed because the convergent ablator data are typically taken about 100 $\mu$m before peak velocity. This is because x-ray self-emission of the core gets brighter close to peak velocity and makes the measurement more difficult. This correction is based on calculations that show that the velocity at this radius is about 2% lower than the actual peak velocity.

The second correction connects the center of mass velocity (the quantity measured in the convergent ablator experiment) with the fuel velocity. This correction depends on the amount of mass remaining.[13,28] Calculations are used to find the correction as a function of mass remaining—it is generally a correction on the order of 10%–13% to the velocity.

The final correction is adjusted for the detailed laser power, energy, and capsule mass for a given DT experiment. This correction is made using the measured time of peak x-ray or neutron emission ("bangtime"). This correction is based on calculations that show that 100 ps in bangtime corresponds to about 3% in velocity. For each experiment, these corrections are made to calculate the implosion velocity.

Figure 11 shows the inferred fuel velocity plotted against $\tilde{v} \sim \sqrt{E_{Au}A/m}$. We see that our fastest implosions have velocities in excess than 350 km/s. (We also note that the two "coasting" implosions do not fall on the same curve and are excluded from the fit.) There is also a power law dependence between $\tilde{v} \sim \sqrt{E_{Au}A/m}$ and implosion velocity. By fitting the data, we find that the implosion velocity, $v \sim \tilde{v}^{1.36}$. Combining this fit with our previous fit of the data suggests the following scalings of neutron yield with implosion velocity:

$$Y \sim \tilde{v}^{11} \sim v^{8},$$

for all shots. If we exclude the lowest yield shot (which had a coasting pulse and low yield)

$$Y \sim \tilde{v}^{12.75} \sim v^{9.4}.$$

If we consider only the highest performing shots (only 5 shots), we find

$$Y \sim \tilde{v}^{15.75} \sim v^{11.6}.$$

For implosions without alpha heating, Betti determined the following scaling:[29]

$$Y_{no\,\alpha} \sim T_{ion,no\,\alpha}^{4.7},$$

where $Y_{no\,\alpha}$ is the yield without alpha heating and $T_{ion,no\,\alpha}$ is the ion temperature also without alpha heating. Betti finds that $T_{ion,no\,\alpha}$ scales with implosion velocity as

$$T_{ion,no\,\alpha} \sim v^{1.25}.$$

Combining these relations, we expect that implosions without alpha heating the yield will scale like

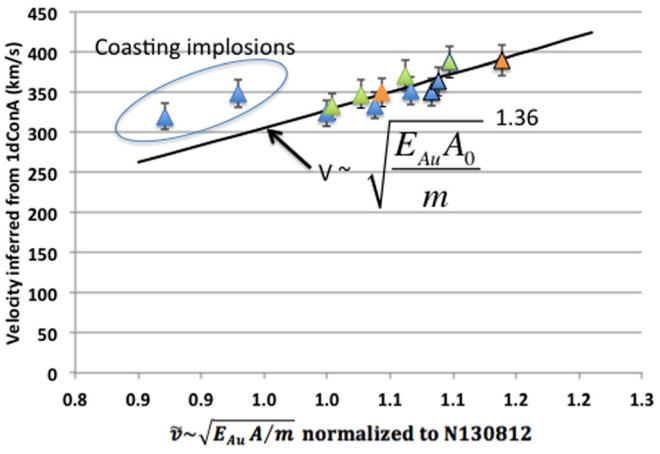


FIG. 11. Implosion velocities inferred from convergent ablator experiments and then scaled to each DT implosion shot show dependence of velocity on our velocity like parameter: $v \sim \tilde{v}^{1.36}$.

$$Y_{no\,\alpha} \sim v^{5.9}.$$

Our look at the collection of high foot data suggests that the velocity exponent increases as we increase the amount of alpha heating. This suggests that looking at the data as a collection is another method for inferring the amount of alpha heating in our implosions.

Using the same relation, we find that the ion temperatures also empirically scale faster than Betti's scaling without alpha heating

$$T_{ion,DD} \sim \tilde{v}^{2.25} \sim v^{1.65},$$
$$T_{ion,DT} \sim \tilde{v}^{2.8} \sim v^{2}.$$

As a cross-check to the simulation-based models, a dynamic model can be used to infer the amount of alpha heating.[30] In this model, the high-density fuel is a piston that supplies PdV work and mass to the hotspot. If we initiate "initial" conditions after peak velocity for the fuel (mass and velocity) and hotspot (mass, temperature, and radius), we can evolve the equation of motion of the inner radius of the fuel (which is identical to the hot-spot radius) along with energy conservation in the hotspot (including losses from radiation and electron conduction as well as heating via alpha particle deposition) and mass conservation (taking into account the increase in hotspot mass due to heating of the fuel by both conduction and alpha particle deposition) to find conditions at stagnation. These conditions can then be compared with hotspot conditions at stagnation that are inferred from the data and a static hotspot model.[31] The initial conditions can then be iterated until the stagnation conditions are consistent with the static model (e.g., hot-spot density, stagnation pressure, etc.) and burn-averaged data such as yield and ion-temperature. Alpha deposition terms in the differential equations can then be turned off in the dynamic model to assess the impact of alpha heating on the dynamics.

Two interesting things come out of this model. First is that the model does not find a self-consistent set of conditions if the DT ion temperature is used, but does find a consistent set if the DD ion temperature is used. As a result, this analysis uses the DD ion temperature. This is likely a reflection of the DT ion temperature being less representative of the real thermal temperature. DD ion temperatures have been measured to be consistently lower than the DT ion temperature by more than the expected ~300 eV difference throughout the high-foot campaign—the leading speculation for this observation is non-radial motions enhancing the measured ion temperature for which the DT measurement is more sensitive.

Second, the model also shows that the yield increasing with an increasing velocity exponent is a function of the amount of alpha heating. Figure 12 shows the yield velocity exponent from the model as a function of the yield multiplication due to alpha heating. If we compare this with the fits to the data above, this suggests that for our entire dataset, we have a yield amplification of about 1.45× (velocity exponent of 8). If we exclude our lowest performing shot (which had a coasting pulse and low yield), then we have an average yield

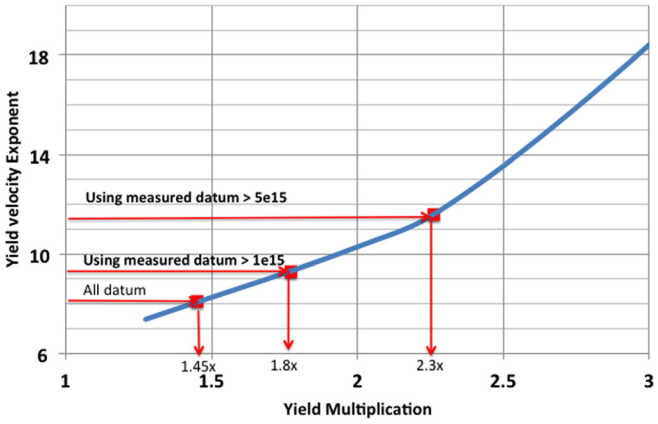


FIG. 12. Dynamic model shows that the yield velocity exponent should increase as alpha heating increases. Comparing this model with the fits to the dataset suggest that we have an average alpha heating of 1.8× for all shots with primary yield $>1 \times 10^{15}$ and amplification of 2.3× for the highest performing 5 shots.

amplification of 1.8× (velocity exponent of 9.4). Our highest performing five shots have a yield amplification of 2.3× (velocity exponent of 11.6). This model, combined with the dataset, provides another method for estimating the alpha heating that is complimentary to the more simulation-based methods of inferring alpha heating.

## V. CONCLUSIONS

We have increased the implosion velocity for the high foot design using the three major components of the ICF system—the laser (higher laser energy and power), the hohlraum (using depleted uranium hohlraums that have higher opacity and lower specific heat to provide more drive for the same laser energy and power), and the capsule (by thinning the capsule to have less mass to push with the same drive). We find that the capsule performance metrics (yield and ion temperature) increase in a very systematic way with a velocity-like parameter, $\tilde{v} \sim \sqrt{E_{Au}A/m}$. This data show that we have achieved the goal of having an implosion that behaves in a predictable way.

Once we had a predictably performing capsule, another goal was to push the design until we found a "cliff" in performance. Finding out how the capsule fails is an important component in understanding the implosion and learning how to optimize the design for ignition. By pushing the thinnest capsule (165 $\mu$m thick ablator compared to the nominal 195 $\mu$m thick ablator) with 1.77 MJ in a uranium hohlraum, we found that the yield was reduced compared with the scaling from the other shots in the dataset. Although we expected to find a cliff due to mix of the ablator into the hotspot, we do not see evidence of mix in this shot. Instead, it seems that we have burned through the capsule ablator. Burn-through of the ablator may have been enhanced by thin spots in the shell due to the capsule support tent and a defect in this particular capsule.[32] Future experiment will explore the cliff further by repeating that experiment with a small reduction in laser energy.

By looking at the dataset as a whole, we find that the yield and ion temperature scale as a high power of implosion velocity. Looking at our complete dataset, we find that the yield scales like $v^8$. If we look at all experiments with primary neutron yield $>1 \times 10^{15}$ (all but the lowest performing shot), then we find that yield scales like $v^{9.4}$. If we only consider the five highest performing shots, then we find a scaling of $v^{11.6}$. In the absence of alpha heating, we expect the "no alpha" yield to scale as $v^{5.9}$. This data suggest that the velocity exponent scaling increases with additional alpha heating. A dynamic model of the fuel and hotspot suggests that these velocity exponents correspond to an average alpha heating of 1.45× (entire dataset), 1.8× (experiments with primary yield $>1 \times 10^{15}$), and 2.3× (5 highest performing shots). Looking at the dataset as a whole (as opposed to looking at individual shots) gives further evidence that we have significant alpha heating in these implosions.

Future directions for this campaign will include working on the other major factors in ICF—increased compression (via a lower adiabat implosion) and improved implosion shape. We have begun to explore implosions that use a high picket version of the low foot, 4-shock pulse to keep ablation front growth low while allowing for improved compression.[33] As we improve compression, we expect that implosion shape will become more important—a campaign to develop a rugby-shaped hohlraum[34] is also underway as a method for improving control over the conventional cylindrical hohlraum.

## ACKNOWLEDGMENTS

This work was performed under the auspices of the U.S. Department of Energy by Lawrence Livermore National Laboratory under Contract No. DE-AC52-07NA27344.

[1]T. R. Dittrich, O. A. Hurricane, D. A. Callahan, E. L. Dewald, T. Doeppner, D. E. Hinkel, L. F. Berzak Hopkins, S. LePape, T. Ma, J. L. Milovich, J. C. Moreno, P. K. Patel, H.-S. Park, B. A. Remington, and J. D. Salmonson, Phys. Rev. Lett. **112**, 055002 (2014).
[2]H.-S. Park, O. A. Hurricane, D. A. Callahan, D. T. Casey, E. L. Dewald, T. R. Dittrich, T. Doeppner, D. E. Hinkel, L. F. Berzak Hopkins, S. LePape, T. Ma, P. K. Patel, B. A. Remington, H. F. Robey, J. D. Salmonson, and J. L. Kline, Phys. Rev. Lett. **112**, 055001 (2014).
[3]O. A. Hurricane, D. A. Callahan, D. T. Casey, P. M. Celliers, C. Cerjan, E. L. Dewald, T. R. Dittrich, T. Doeppner, D. E. Hinkel, L. F. Berzak Hopkins, J. L. Kline, S. LePape, T. Ma, A. G. MacPhee, J. L. Milovich, A. Pak, H.-S. Park, P. K. Patel, B. A. Remington, J. D. Salmonson, P. T. Springer, and R. Tommasini, Nature **506**, 343 (2014).
[4]O. A. Hurricane, D. A. Callahan, D. T. Casey, E. L. Dewald, T. R. Dittrich, T. Döppner, M. A. Barrios Garcia, D. E. Hinkel, L. F. Berzak Hopkins, P. Kervin *et al.*, Phys. Plasmas **21**, 056314 (2014).
[5]K. S. Raman, V. A. Smalyuk, D. T. Casey, S. W. Haan, D. E. Hoover, O. A. Hurricane, J. J. Kroll, A. Nikroo, J. L. Peterson, B. A. Remington, H. F. Robey, D. S. Clark, B. A. Hammel, O. L. Landen, M. M. Marinak, D. H. Munro, K. J. Peterson, and J. Salmonson, Phys. Plasmas **21**, 072710 (2014).
[6]V. A. Smalyuk, M. Barrios, J. A. Caggiano, D. T. Casey, C. J. Cerjan, D. S. Clark, M. J. Edwards, J. A. Frenje, M. Gatu-Johnson, V. Y. Glebov *et al.*, Phys. Plasmas **21**, 056301 (2014).
[7]D. T. Casey, V. A. Smalyuk, K. S. Raman, J. L. Peterson, L. Berzak Hopkins, D. A. Callahan, D. S. Clark, E. L. Dewald, T. R. Dittrich, S. W. Haan *et al.*, Phys. Rev. E **90**, 011102(R) (2014).
[8]S. W. Haan, J. D. Lindl, D. A. Callahan, D. S. Clark, J. D. Salmonson, B. A. Hammel, L. J. Atherton, R. C. Cook, M. J. Edwards, S. Glenzer *et al.*, Phys. Plasmas **18**, 051001 (2011).
[9]B. K. Spears, S. Glenzer, M. J. Edwards, S. Brandon, D. Clarks, R. Town, C. Cerjan, R. Dylla-Spears, E. Mapoles, D. Munro, J. Salmonson, S. Sepke, S. Weber, S. Hatchett, S. Haan, P. Springer, E. Moses, J. Kline, G. Kyrala, and D. Wilson, Phys. Plasmas **19**, 056316 (2012).

[10]E. L. Dewald, K. M. Campbell, R. E. Turner, J. P. Holder, O. L. Landen, S. H. Glenzer, R. L. Kauffman, L. J. Suter, M. Landon, M. Rhodes, and D. Lee, Rev. Sci. Instrum. **75**, 3759 (2004).
[11]J. L. Kline, D. A. Callahan, S. H. Glenzer, N. B. Meezan, J. D. Moody, D. E. Hinkel, O. S. Jones, A. J. Mackinnon, R. Bennedetti, R. L. Berger *et al*., Phys. Plasmas **20**, 056314 (2013).
[12]A. L. Kritcher, R. Town, D. Bradley, D. Clark, S. Spears, O. Jones, S. Haan, P. T. Springer, J. Lindl, R. H. H. Scott, D. Callahan, M. J. Edwards, and O. L. Landen, Phys. Plasmas **21**, 042708 (2014).
[13]D. A. Callahan, N. B. Meezan, S. H. Glenzer, A. J. Mackinnon, L. R. Benedetti, D. K. Bradley, J. R. Celeste, P. M. Celliers, S. N. Dixit, T. Döppner *et al*., Phys. Plasmas **19**, 056305 (2012).
[14]O. S. Jones, J. Schein, M. D. Rosen, L. J. Suter, R. J. Wallace, E. L. Dewald, S. H. Glenzer, K. M. Campbell, B. A. Hammel, O. L. Landen, C. M. Sorce, R. E. Olson, G. A. Rochau, H. L. Wilkins, J. L. Kaae, J. D. Kilkenny, A. Nikroo, and S. P. Regan, Phys. Plasmas **14**, 056311 (2007).
[15]T. Doeppner, D. A. Callahan, O. A. Hurricane, D. E. Hinkel, T. Ma, H.-S. Park, L. F. Berzak Hopkins, D. T. Casey, P. Celliers, E. L. Dewald *et al*., "Demonstration of improved performance of fully-integrated deuterium-tritium capsule implosions in depleted uranium hohlraums on NIF," Phys. Rev. Lett. (submitted).
[16]P. A. Michel, S. H. Glenzer, L. Divol, D. K. Bradley, D. Callahan, S. Dixit, S. Glenn, D. Hinkel, R. K. Kirkwood, J. L. Kline, W. L. Kruer, G. A. Kyrala, S. LePape, N. B. Meezan, R. Town, K. Widmann, E. A. Williams, B. J. MacGowan, J. Lindl, and L. J. Suter, Phys. Plasmas **17**, 056305 (2010).
[17]S. W. Haan, M. C. Herrmann, T. R. Dittrich, A. J. Fetterman, M. M. Marinak, D. H. Munro, S. M. Pollaine, J. D. Salmonson, G. L. Strobel, and L. J. Suter, Phys. Plasmas **12**, 056316 (2005).
[18]T. Ma, O. A. Hurricane, D. A. Callahan, M. A. Barrios, D. T. Casey, E. L. Dewald, T. R. Dittrich, T. Döppner, S. W. Haan, D. E. Hinkel *et al*., "Thin shell, high velocity ICF implosions on the National Ignition Facility," Phys. Rev. Lett. **114**, 145004 (2015).
[19]T. Ma, P. K. Patel, N. Izumi, P. T. Springer, M. H. Key, L. J. Atherton, L. R. Benedetti, D. K. Bradley, D. A. Callahan, P. M. Celliers *et al*., Phys. Rev. Lett. **111**, 085004 (2013).
[20]C. Cerjan, D. B. Sayre, O. L. Landen, J. A. Church, W. Stoeffl, E. M. Grafil, H. W. Herrmann, N. M. Hoffman, and Y. Kim, "Gamma reaction history diagnostic determination of ablator areal density in NIF implosion experiments," Phys. Plasmas **22**, 032710 (2015).
[21]T. Ma, N. Izumi, R. Tommasini, D. K. Bradley, P. Bell, C. J. Cerjan, S. Dixit, T. Doeppner, O. Jones, J. L. Kline, G. Kyrala, O. L. Landen, S. LePape, A. J. Mackinnon, H.-S. Park, P. K. Patel, R. R. Prasad, J. Ralph, S. P. Regan, V. A. Smalyuk, P. T. Springer, L. Suter, R. P. J. Town, S. V. Weber, and S. H. Glenzer, Rev. Sci. Instrum. **83**, 10E115 (2012).
[22]N. Izumi, T. Ma, M. Barrios, L. R. Benedetti, D. Callahan, C. Cerjan, J. Edwards, S. Glenn, S. Glenzer, J. Kilkenny, J. Kline, G. Kyrala, O. L. Landen, S. Regan, P. Springer, L. Suter, R. Tommasini, R. Town, A. J. Mackinnon, P. Bell, and D. K. Bradley, Rev. Sci. Instrum. **83**, 10E121 (2012).
[23]S. R. Nagel, S. W. Haan, J. R. Rygg, C. Aracne-Ruddle, M. Barrios, *et al*., Phys of Plasmas **22**, 022704 (2015); **22**, 039902 (2015).
[24]T. J. Murphy, Phys. Plasmas **21**, 072701 (2014).
[25]B. K. Spears, D. H. Munro, S. Sepke, J. Caggiano, D. Clark, R. Hatarik, A. Kritcher, D Sayre, C. Yeamans, J. Knauer, T. Hilsabeck, and J. Kilkenny, "Three-dimensional simulations of National Ignition Facility implosions: Insight into experimental observables," Phys. Plasmas (this issue – to be published).
[26]D. G. Hicks, N. B. Meezan, E. L. Dewald, A. J. Mackinnon, R. E. Olson, D. A. Callahan, T. Döppner, L. R. Benedetti, D. K. Bradley, P. M. Cellier *et al*., Phys. Plasmas **19**, 122702 (2012).
[27]J. R. Rygg, O. S. Jones, J. E. Field, M. A. Barrios, L. R. Benedetti, G. W. Collins, D. C. Eder, M. J. Edwards, J. L. Kline, J. J. Kroll, O. L. Landen, T. Ma, A. Pak, J. L. Peterson, K. Raman, R. P. J. Town, and D. K. Bradley, PRL **112**, 195001 (2014).
[28]N. B. Meezan, A. J. MacKinnon, D. G. Hicks, E. L. Dewald, R. Tommasini, S. LePape, T. Döppner, T. Ma, D. R. Farley, D. H. Kalentar *et al*., Phys. Plasmas **20**, 056311 (2013).
[29]R. Betti, P. Y. Chang, B. K. Spears, K. S. Anderson, J. Edwards, M. Fatenejad, J. D. Lindl, R. L. McCrory, R. Nora, and D. Shvarts, Phys. Plasmas **17**, 058102 (2010).
[30]O. A. Hurricane, D. A. Callahan, D. T. Casey, E. L. Dewald, T. R. Dittrich *et al*., "Alpha-particle self-heating dominated inertially confined fusion plasmas," Nat. Phys. (submitted).
[31]C. Cerjan, P. T. Springer, and S. M. Sepke, Phys. Plasmas **20**, 056319 (2013).
[32]R. Bionta, private communication (2014).
[33]D. S. Clark, J. L. Milovich, D. E. Hinkel, J. D. Salmonson, J. L. Peterson, L. F. Berzak Hopkins, D. C. Eder, S. W. Haan, O. S. Jones, M. M. Marinak, H. F. Robey, V. A. Smalyuk, and C. R. Weber, Phys. Plasmas **21**, 112705 (2014).
[34]P. Amendt, J. S. Ross, J. L. Milovich, M. Schneider, E. Storm, D. A. Callahan, D. Hinkel, B. Lasinski, D. Meeker, P. Michel, J. Moody, and D. Strozzi, Phys. Plasmas **21**, 112703 (2014).